

Hydrogen-bond fluctuations of the hydration shell of the bromide anion

R. L. A. Timmer,^{*} and H. J. Bakker

FOM-institute for Atomic and Molecular Physics, Kruislaan 407, 1098 SJ Amsterdam, The Netherlands

E-mail: r.timmer@amolf.nl

Abstract

We study the hydrogen-bond dynamics of solutions of LiBr and NaBr in isotopically diluted water (2% HDO:D₂O) with femtosecond spectral hole-burning spectroscopy. We study the frequency fluctuations of the O–H stretch vibrations of the HDO molecules and observe spectral dynamics with time constants of 0.8 ± 0.1 ps and 4.3 ± 0.3 ps. The slow process we assign to the hydrogen-bond fluctuations of the O–H \cdots Br[−] hydrogen bonds of the hydration shell of the Br[−] anion. We find that the time scale of the hydrogen-bond fluctuations of the hydration shell of Br[−] is independent of the nature of the cation and the concentration.

The fluctuations of the hydrogen-bond network of liquid water play an essential role in many chemical processes occurring in this liquid.^{1,2} Hence, there exists a strong interest in the rate and nature of these fluctuations in the hydration shells of ions and molecules. With the development of intense femtosecond mid-infrared laser pulses it has become possible to study the hydrogen-bond fluctuations of water directly in the time domain using nonlinear vibrational spectroscopic techniques. Over the last years these techniques combined with molecular dynamics (MD) simulations have provided new information on the hydrogen bond dynamics in pure liquid water.^{3–16}

Nonlinear vibrational spectroscopic studies of the hydrogen-bond dynamics of water make use of the fact that the frequency and absorption cross-section of the high-frequency intramolecular O–H stretch vibrations of the water molecules are sensitive probes of the strength of the intermolecular hydrogen-bond interactions. A strengthening of the hydrogen bond that is donated by the O–H group to another molecule or ion, leads to a decrease of the frequency of the O–H stretch vibration.¹⁷ Hence, fluctuations in the strengths of the local donated hydrogen bonds are directly observable as time-dependent frequency shifts of the O–H stretch vibrations. These spectral fluctuations can be characterized by a frequency-frequency correlation function (FFCF) $\langle \delta\omega(t)\delta\omega(0) \rangle$.

Ions have a strong effect on the hydrogen-bond structure of liquid water. The strong electric fields exerted by the ions disrupt the local hydrogen-bond structure and orient nearby water molecules depending on their charges, leading to the formation of so-called hydration shells. For solutions containing halide anions, new types of hydrogen bonds between water and the ions are formed. These O–H \cdots X[−] (X[−] = F[−], Cl[−], Br[−]) hydrogen bonds are directional in character,^{18,19} which means that the O–H bond and the O \cdots X[−] hydrogen-bond coordinates are collinear.

In earlier work we studied the hydrogen-bond fluctuations of the hydration shells of ions with two-color pump-probe spectroscopy.^{20,21} We found the time constants of the decay of the FFCF of the hydration shells to be quite long, ranging from 10 to 25 ps. In a recent study by Park et al. the frequency fluctuation dynamics of NaBr solutions were measured with two-dimensional vibrational echo spectroscopy. The FFCF measured for solutions of different concentration were fitted with three time constants that represent various contribution to the structural evolution of the water-ion systems. The slowest component was observed to show the strongest slowing down with concentration, reaching a maximum value of 4.8 ps for a solution of 6 M NaBr. The slowing down of this component was assigned to a decrease of the rate of the global structural rearrangement of the liquid that follows from the increasing number of hydrogen bonds to Br[−] ions. Here we present a study of the hydrogen-bond fluctuations of solutions containing bromide ions using femtosecond infrared spectral hole-burning spectroscopy. In comparison to the earlier femtosecond infrared studies^{20–23} we measure the spectral dynamics at higher concentrations and over a longer time

R. L. A. Timmer et al. Hydrogen-bond fluctuations of the hydration shell of the bromide anion scale. As a result, we obtain detailed and highly specific information on the hydrogen-bond dynamics of the hydration shells of the Br^- ions. We study the dependence of these dynamics on the concentration and the nature of the cation. We discuss the results in relation to earlier experimental and theoretical work on this system.

Experimental

The dynamics of the O–H stretch vibrations of HDO in the hydration shells of bromide ions are studied with femtosecond spectral hole-burning spectroscopy. The femtosecond mid-infrared pump and probe pulses are generated via a sequence of nonlinear frequency-conversion processes. As a first step in the generation of the pump pulses we generate pulses with wavelengths of ~ 1250 nm (signal) and ~ 2200 nm (idler) via optical parametric generation and amplification in BBO (β -bariumborate) (Light-Conversion TOPAS). This process is pumped by pulses with a central wavelength of 800 nm, a pulse duration 100 fs, and an energy of 0.7 mJ per pulse. This energy constitutes a fraction of 2.8 mJ pulses delivered by a 1 kHz regenerative and multi-pass Ti:sapphire amplifier (Quantronix Titan). In a second BBO crystal, the idler pulses at ~ 2200 nm are frequency doubled to pulses with a wavelength of ~ 1100 nm that are subsequently used as seed in a parametric amplification process in a potassium-titanyl-phosphate (KTP) crystal. The latter process is pumped with 800 nm pulses with an energy of 1 mJ, representing another fraction of the output of the Ti:sapphire regenerative and multi-pass amplifiers. The parametric amplification in the KTP crystal leads to amplification of the ~ 1100 nm seed pulses and to the generation of light at a wavelength of ~ 3000 nm with an energy of $10 \mu\text{J}$. The duration of the latter pulses is 150 fs and the bandwidth is 70 cm^{-1} . The central frequency of the pump can easily be changed by rotating the crystals.

The probe pulses are generated in a separate sequence of nonlinear frequency-conversion processes. The first process of this sequence is white-light seeded optical parametric amplification in BBO (SpectraPhysics OPA). The white light generation and parametric amplification processes

are pumped with 800 nm pulses with a total energy of 0.5 mJ, representing another fraction of the output of the Ti:sapphire regenerative and multi-pass amplifier. The parametric amplification results in pulses with wavelengths of ~ 1250 nm (signal) and ~ 2200 nm (idler). The signal and idler are used as input in a difference-frequency mixing process in AgGaS₂, which implies that the idler is amplified using the signal as pump. In this process a pulse is generated with a wavelength of ~ 3000 nm, a pulse duration of 100 fs, an energy of 1 μ J, and a frequency bandwidth of 200 cm^{-1} . The probe can be tuned independently from the pump pulse.

The pump and probe pulses are used in spectral hole burning experiments on aqueous solutions of LiBr and NaBr. LiBr can be dissolved up to 177 g per 100 ml water, NaBr up to 73 g per 100 ml water. The concentrations studied are 5, 10 and 15 molal for the LiBr solutions and 6 molal for the NaBr solution. For all solutions the solvent was a solution of 2% HDO in D₂O. This concentration is sufficiently low to avoid the measurements to be affected by resonant energy transfer between O–H vibrations located on different HDO molecules.²⁴ In principle, the hydrogen-bond dynamics of solutions of the Br[−] anion can also be studied by probing the response of the O–D stretch vibration of HDO molecules dissolved in H₂O. However, in that case relatively high concentrations of HDO have to be used because the H₂O solvent gives a strong background signal in the absorption region of the O–D stretch vibration. As a result, the vibrational relaxation results in a relatively strong thermal signal. For the O–H stretch vibration of HDO in D₂O, the corresponding background signal is much smaller, so that lower concentrations can be used which results in a much smaller thermal signal after the relaxation is complete.

The sample is contained in a cell with CaF₂ windows and an optical path length of 200 μ m. The pump pulse excites a few percent of the O–H vibration from the $\nu = 0$ ground state to the $\nu = 1$ excited state. This excitation leads to a bleaching effect at the fundamental transition frequency, due to a decrease of the $\nu = 0 \rightarrow 1$ absorption and $\nu = 1 \rightarrow 0$ stimulated emission. As the absorption spectrum of the O–H stretch vibration is inhomogeneously broadened, the bleaching has the form of a spectral hole in the absorption band. The shape of the spectral hole evolves in time due to spectral fluctuations. The dynamics of the shape of the spectral hole are monitored with the

broadband probe pulse.

The pump pulses are focussed in the sample using a CaF_2 lens with a focal length of 10 cm to a focus with a diameter of 100 μm . The probe pulses are sent on a wedged CaF_2 plate. The front side reflection ($\sim 5\%$) is focussed within the focal volume of the pump pulse using a CaF_2 lens with a focal length of 7.5 cm. The probe light transmitted through the sample is dispersed with an Oriel monochromator and detected with one line of an Infrared Associates 2×32 MCT (mercury-cadmium-telluride) detector array. The reflection from the back side of the wedged CaF_2 plate is also focussed in the sample, but not in overlap with the pump. This fraction is also dispersed by the monochromator and detected by the second line of the MCT detector array. This signal is used as a reference in the experiment to enable a frequency-resolved correction for shot-to-shot fluctuations in the probe-pulse energy.

Results

Figure 1 shows the linear absorption spectrum of the O–H stretch vibration of HDO molecules for pure HDO:D₂O and for solutions of 5 molal and 15 molal LiBr dissolved in HDO:D₂O. The absorption spectrum of the salt solution is blueshifted with respect to the absorption spectrum of pure HDO:D₂O. This blueshift has been observed before for solutions containing Cl^- , Br^- and I^- ions, and shows that the average hydrogen bond strength decreases upon the addition of these ions. The absorption spectrum of aqueous solutions containing these halide anions can be decomposed in two distinct subbands.¹⁹ The first of these subbands corresponds to O–H groups of HDO molecules that are hydrogen bonded to the oxygen atom of nearby D₂O molecules, thus forming O–H \cdots O hydrogen-bonded systems. This subband is very similar to the absorption spectrum of pure HDO:D₂O. The second subband is associated with HDO molecules of which the O–H group is hydrogen bonded to X^- ($\text{X}^- = \text{Cl}^-$, Br^-),^{19,21} thus forming O–H \cdots X^- hydrogen-bonded systems. The latter subband is narrower and is blueshifted in comparison to the O–H \cdots O subband.

In Figure 2 transient spectra are shown, measured at different delay times between pump and

probe, for a solution of 5 molal lithium bromide in HDO:D₂O. For frequencies above ~ 3300 cm⁻¹ the spectra show the bleaching of the fundamental $\nu = 0 \rightarrow 1$ absorption and $\nu = 1 \rightarrow 0$ stimulated emission. At frequencies below ~ 3300 cm⁻¹, the spectra show the presence of excited state $\nu = 1 \rightarrow 2$ absorption. The relaxation of the $\nu = 1$ state leads to a decay of both the bleaching and the excited-state absorption signal. The relaxation also results in a small temperature increase of the sample in the focus of the pump laser. Due to this increase in temperature, the transient spectral changes do not decay to zero, but evolve to a characteristic small-amplitude transient spectrum that does not decay on the picosecond time scale of the experiment. For the transient spectra shown in Figure 2, the ingrowing heating spectrum has been subtracted, so that these spectra only represent the transient absorption changes associated with the excitation of the $\nu = 1$ state.²⁵ The rate at which this heating signal grows in, is the same as the vibrational relaxation rate, i. e. bi-exponential with time constants equal to the T_1 values of bulk and bromide bound water. The bleaching part of the spectrum is narrower than the linear absorption spectrum, which shows that the pump has excited a spectral hole in the inhomogeneously broadened absorption band. With increasing delay both the bleaching and the induced absorption signal shift to higher frequencies.

In Figure 3 the maximum of the bleaching signal is presented as a function of delay time for the three different LiBr solutions. For all solutions of LiBr, the signal shows a clear bi-exponential decay. The amplitude of the slow component increases with the concentration of dissolved salt, showing that this component results from water molecules interacting with the salt ions. The fast component of the relaxation has a time constant of 0.8 ± 0.1 ps for all three solutions. We assign this component to the relaxation of the O–H groups forming an O–H \cdots O hydrogen bond to D₂O. The observed time constant agrees with the value of T_1 that has been observed before for the O–H stretch vibration of pure HDO:D₂O.²⁶ The slow component is assigned to the vibrational relaxation of O–H groups forming O–H \cdots Br⁻ hydrogen bonds to Br⁻ ions. Its time constant depends slightly on the concentration of dissolved salt. For the solutions studied of 5, 10 and 15 molal LiBr, the value of T_1 is 3.1 ± 0.2 ps, 3.6 ± 0.2 ps, and 3.8 ± 0.2 ps, respectively.

The signals shown in Figure 2 reflect the vibrational relaxation and frequency fluctuations of

both the O–H···O and O–H···Br[−] subbands. However, thanks to the difference in vibrational lifetime, the transient spectrum will become completely dominated by the O–H···Br[−] subbands for delays >4 ps. Hence, we can obtain highly specific information on the spectral dynamics of the O–H···Br[−] oscillators by monitoring the spectral dynamics at these longer delay times. In Figure 4 transient spectra are shown at three different long delay times for a solution of 15 molal LiBr in HDO:H₂O. In the top panel the pump pulse is tuned to 3310 cm^{−1}, in the red wing of the absorption band. The lower panel represents the case where the pump pulse was centered at 3550 cm^{−1}, in the blue wing of the absorption band. The transient spectra observed at a delay of 4 ps in the upper and lower panel are shifted with respect to each other, which shows that the O–H···Br[−] subband is inhomogeneously broadened. With increasing delay, the transient spectra broaden and the central frequency of the spectra shifts to a value of 3450 cm^{−1}. In Figure 5 the spectra of the top panel of Figure 4 are shown normalized to illustrate more clearly the effect of the spectral diffusion within the O–H···Br[−] subband. At a delay of 12 ps, the shapes of the spectral holes obtained with blue and red pumping have become indistinguishable (Figure 4), showing that the spectral diffusion is complete.

To obtain more detailed information on the spectral diffusion dynamics, we determine the first moment of the bleaching of the transient spectra as a function of delay time. To determine the first moment we first determine the frequency of the zero crossing between the bleaching and the excited state absorption with great accuracy. We fit the transient spectra to two gaussians representing the bleaching and the excited state absorption. From the fit we obtain the frequency ν_{zc} at which the transient absorption change equals zero for a given delay and central pump frequency. To determine the first moment, we integrate the fitted bleaching starting from the frequency ν_{zc} of the zero crossing to the highest frequency ν_{up} of 3700 cm^{−1} of the measured frequency interval:

$$S_1(\tau) = \frac{\int_{\nu_{zc}}^{\nu_{up}} \nu \Delta\alpha(\nu, \tau) d\nu}{\int_{\nu_{zc}}^{\nu_{up}} \Delta\alpha(\nu, \tau) d\nu} \quad (1)$$

In Figure 6 the resulting first moments are shown for solutions of 5 and 15 molal LiBr in

HDO:D₂O. It is seen that for both solutions the first moments converge to the same central frequency $\nu_{c,\text{OH-Br}}$. The dynamics can be fitted well with the following bi-exponential function:

$$S_{1,\text{fit}}(\tau) = \nu_{c,\text{OH-Br}} + A_1 e^{-\tau/\tau_1} + A_2 e^{-\tau/\tau_2} \quad (2)$$

with the same time constants τ_1 and τ_2 for red pumping ($\nu_{\text{pu}}=3310 \text{ cm}^{-1}$) and blue pumping ($\nu_{\text{pu}}=3550 \text{ cm}^{-1}$).

We also determined the dynamics of the first moment of the bleaching of the transient absorption spectra measured for a solution of 6 molal NaBr in HDO:D₂O. The first moments obtained with red and blue pumping again show the same bi-exponential dynamics and converge to the same central frequency. The time constants obtained from a simultaneous fit to the first moments obtained with red and blue pumping are shown in Table 1.

Interpretation

The fast component of the dynamics of the first spectral moment with a time constant of $0.8 \pm 0.1 \text{ ps}$ is important in the first few picoseconds after the excitation. This fast component contains several contributions. It contains the vibrational population decay of the excited O–H···O oscillators. The spectral response of these oscillators differs from that of the longer-living excited O–H···Br[−] oscillators. Hence, the decay of the O–H···O subband leads to spectral dynamics with a time constant corresponding to the vibrational lifetime of the O–H···O vibrations. The fast spectral dynamics can also contain a contribution of spectral diffusion within the O–H···O subband. For bulk HDO:D₂O it was found that the FFCF contains a fast part with a time constant of $\sim 100 \text{ fs}$ and a slow part with a time constant of $\sim 1 \text{ ps}$.^{3–15} The slow component of the FFCF has been described with a single time constant with a value of $\sim 1 \text{ ps}$ ^{3–5,7–12,14,15} or with two time constants of $\sim 0.4 \text{ ps}$ and $\sim 1.8 \text{ ps}$.¹³ The slow part of the spectral diffusion of the O–H···O oscillators may well contribute to the fast component with a time constant of $\sim 0.8 \text{ ps}$ observed for the LiBr and NaBr solutions. Finally, the fast component of the observed spectral dynamics can contain a fast

R. L. A. Timmer et al. Hydrogen-bond fluctuations of the hydration shell of the bromide anion

component of the spectral dynamics of the $\text{O-H}\cdots\text{Br}^-$ oscillators. For an HDO molecule for which the O-H group is hydrogen bonded to Br^- , the O-D group will likely be bonded to the oxygen atom of a D_2O molecule. The FFCF of this $\text{O-D}\cdots\text{O}$ system will show a component with a time constant of ~ 1 ps and the corresponding hydrogen-bond fluctuations may well affect the $\text{O-H}\cdots\text{Br}^-$ hydrogen-bond and thus the O-H frequency at the other side of the HDO molecule. In that case the spectral dynamics of the $\text{O-H}\cdots\text{Br}^-$ oscillators will also show a contribution of the $\text{O-D}\cdots\text{O}$ hydrogen-bond fluctuations. The fast component will likely not contain a contribution of the exchange between $\text{O-H}\cdots\text{Br}^-$ and $\text{O-H}\cdots\text{O}$ oscillators, i. e. a switching of hydrogen bonds between the hydration shell and the surrounding liquid. In a recent study of the spectral dynamics of NaBF_4 solutions it was shown that this exchange takes place on a substantially longer time scale of ~ 7 ps.²⁷

From the values shown in Table 1 it follows that the relative amplitude of the fast component strongly decreases with increasing salt concentration, especially in the case of pumping in the red wing of the absorption band. Because the contribution of $\text{O-H}\cdots\text{O}$ to the signal decreases with increasing concentration, this result indicates that the fast component in the dynamics of the first spectral moment is dominated by the $\text{O-H}\cdots\text{O}$ component and does not represent a fast component of the spectral dynamics of the $\text{O-H}\cdots\text{Br}^-$ subband. Moreover, in the case of pumping in the red wing, the ratio A_1/A_2 is larger than in the case of pumping in the blue wing. As the $\text{O-H}\cdots\text{O}$ subband is redshifted with respect to the $\text{O-H}\cdots\text{Br}^-$ subband, this result also indicates that the fast component in the dynamics of the first spectral moment is associated with dynamics of the $\text{O-H}\cdots\text{O}$ subband. The fast component is likely dominated by the vibrational relaxation of the $\text{O-H}\cdots\text{O}$ subband, because the time constant of this component of 0.8 ± 0.1 agrees very well with the value of T_1 of the excited $\text{O-H}\cdots\text{O}$ and because the transient spectra at early delay times clearly show the decay of the $\text{O-H}\cdots\text{O}$ subband (Figure 2).

For the solution of 15 molal LiBr the ratio A_1/A_2 is smaller for red pumping than for blue pumping. This indicates that at this very high concentration the absorption spectrum of the hydration shell of Br^- possesses a strong red wing. In the linear absorption spectrum of Figure 1

it is seen that for a solution of 15 molal LiBr the absorption spectrum has a slightly stronger red absorption wing than for a solution of 5 molal LiBr (Figure 1). Here it should also be realized that the amplitude of the O–H···O subband will be significantly lower for a 15 molal LiBr solution than for a 5 molal LiBr solution. The fact that nevertheless the absorption spectrum shows a slight redshift going from a 5 molal to a 15 molal solution shows that for the latter solution the O–H···Br[−] subband must indeed possess a stronger red wing. This red wing is likely due to the fact that at this high concentration the Li⁺ ions will be close to the hydration shell of the Br[−] ions, thus forming Li⁺O–H···Br[−] hydrogen-bonded systems. The high charge density of the Li⁺ ion polarizes the O–H···Br[−] hydrogen bond, leading to a strengthening of this bond and a redshift of the corresponding O–H stretch frequency.

We find that the time constant of the fluctuations of the O–H···Br[−] hydrogen bonds is not very much dependent on the concentration of dissolved salt and also not very much dependent on the nature of the cation. This indicates that the dynamics of the hydration shell are relatively uncoupled from the dynamics of the rest of the water network. For bulk water the FFCF shows time constants of ~ 100 fs and ~ 1 ps, significantly slower than the fluctuations of the hydration shell of Br[−]. This large difference in time scales probably explains why the dynamics of the hydration shell are not strongly coupled to the rest of the liquid. The comparison of solutions of LiBr and NaBr shows that the nature of the cation has very little effect on the time constant of the O–H···Br[−] fluctuations.

Discussion

In an earlier study we have measured the dynamics of the hydration shells of the halide anions Cl[−], Br[−] and I[−] with two-color femtosecond pump-probe spectroscopy.^{20,21} In these studies the time constants for the spectral diffusion of the hydration shells were derived from the dependence of the decays of the signals on the pump and probe frequencies. It was observed that the decay became slower when the probe frequency was increasingly detuned from the pump, showing the presence of a slow spectral diffusion process. The determination of the time constants of the

spectral diffusion relied on the modeling of these spectral dynamics. Using a Brownian oscillator model we arrived at time constants ranging from 10-25 ps.^{20,21} In the present study we directly monitor the dynamics of the spectral holes burned by the excitation pulse using a broadband probe pulse. This method does not require any modeling of the spectral dynamics, and we obtain a much more accurate determination of the spectral diffusion dynamics. We now find that the time constant obtained previously were a factor 2-5 too long.

The method used in this study is similar to two-dimensional (2D) vibrational correlation spectroscopy. There are two variations of this type of spectroscopy: double-resonance or dynamic hole burning spectroscopy and pulsed Fourier transform or heterodyne detected vibrational echo correlation spectroscopy. The method used here is the same as double resonance dynamic hole burning spectroscopy. In comparison to heterodyne detected vibrational echo correlation spectroscopy using < 50 fs mid-infrared pulses,^{15,22,23} the present method has as a disadvantage that the spectral dynamics cannot be measured at times < 150 fs after the excitation. An important advantage of the present method is that the pre-selection of particular pump frequencies allows for a high signal-to-noise ratio with the result that we can measure spectral shifts on the order of 1 cm^{-1} up to delay times of 15 ps.

The hydrogen-bond fluctuation dynamics of solutions of NaBr have recently been studied with femtosecond vibrational echo correlation spectroscopy. At the highest concentration studied (6 M) the observed FFCF showed a slow component with a time constant of 4.8 ± 0.6 ps, in good agreement with the 4.3 ± 0.3 ps we observe for the slow component of the FFCF of a solution of 6 molal NaBr. An important difference with the present work is that in the previous work the observed FFCF was assumed to represent the dynamics of all water molecules at all time scales.^{22,23} The slow component was thus assigned to a global restructuring of the solution and was expected to slow down with increasing concentration because of the increasing number of hydrogen bonds to Br^- . However, the assumption that the slow component would represent the dynamics of all water molecules is not valid, because the water hydroxyl groups that form a hydrogen bond to Br^- show a much longer vibrational lifetime than the water hydroxyl groups that

R. L. A. Timmer et al. Hydrogen-bond fluctuations of the hydration shell of the bromide anion form hydrogen bonds to an oxygen atom of another water molecule.^{20–23,28} Hence, with increasing delay time, the measured signal will show an increasing bias to the dynamics of the hydroxyl groups that form a hydrogen bond to Br^- . The slowest time scale of the FFCF will thus represent the spectral fluctuations of the $\text{O-H}\cdots\text{Br}^-$ systems only, i. e. the hydration shells of the Br^- ions. The dynamics of water *outside* the first hydration shell were observed and calculated not to be very different from bulk liquid water.^{29–31}

Recently, the $\text{O-H}\cdots\text{X}^-$ hydrogen bond correlation functions of water in the hydration shell of the halide anions were calculated with molecular dynamics simulations. In these studies a distinction was made between the so-called continuous hydrogen-bond correlation function and the intermittent hydrogen-bond correlation function. The continuous correlation function represents the case where there are no bond breakings in the time interval between 0 and t . For the intermittent case temporary bond breakings are allowed, and the correlation function only decays when the hydrogen bond is broken at time t . The calculated decay time constant for the continuous hydrogen-bond correlation function ranges from 0.5 to 2 ps, depending on the definition of the hydrogen bond.³² The intermittent time constant is ~ 4 ps,³¹ which is very similar to the observed time constant of 4.3 ± 0.3 ps we observe. This indicates that the $\text{O-H}\cdots\text{Br}^-$ hydrogen bond may experience rapid fluctuations including transient breaking and reformation, but the reformation tends to produce the same $\text{O-H}\cdots\text{Br}^-$ hydrogen bond with the same O–H stretch frequency as before the breaking. Hence, these rapid fluctuations do not lead to full spectral equilibration. The full spectral equilibration involves a much slower process, and probably involves a reorganization of the complete hydration shell. Such a complete reorganization can result in two effects. In the first place a new $\text{O-H}\cdots\text{Br}^-$ hydrogen bond can be formed and the corresponding O–H stretch vibrational frequency can be found at a different position in the $\text{O-H}\cdots\text{Br}^-$ absorption subband. Hence, such a complete reorganization will indeed lead to a complete spectral equilibration of the $\text{O-H}\cdots\text{Br}^-$ absorption subband. Second, the reorganization can lead to a rotation of the hydroxyl group out of the hydration shell leading to the formation of a hydrogen bond to another water molecule, i. e. an $\text{O-H}\cdots\text{O}$ hydrogen bond. In this case, the O–H group will show a relatively fast

R. L. A. Timmer et al. Hydrogen-bond fluctuations of the hydration shell of the bromide anion
vibrational relaxation with the result that the O–H oscillator vanishes from the signal.³³

The rotation out of the hydration shell will contribute to the observed vibrational relaxation of the O–H \cdots Br $^-$ oscillators as this rotation turns the slowly relaxing O–H \cdots Br $^-$ system into a rapidly relaxing O–H \cdots O system. Hence, the observed vibrational relaxation rate will be the sum of two channels, one being the intrinsic relaxation of the intact O–H \cdots Br $^-$ system, the other formed by out-of-shell rotation followed by fast relaxation. The fraction of hydroxyl groups that rotate out of the hydration shell upon reorganization will depend on the concentration dissolved salt, as this concentration determines the number density of available water molecules to which a new O–H \cdots O hydrogen bond can be formed. Hence, at high concentrations rotation out of the shell becomes a less likely process, leading to an increase of T_1 , as is indeed observed experimentally.³⁴ The concentration dependence of T_1 can be used to estimate the time constant of the out-off-shell rotation at low concentrations.³⁵ The value of T_1 increases from 2.5 ps for a solution of 1 M LiBr³⁴ to 3.8 ps for a solution of 15 m LiBr. If we assume that the out-off-shell rotation is completely switched off at high concentrations, it follows that $\tau_{\text{os}}(\text{Br}^-) = 1/[(1/2.5) - (1/3.8)] \approx 7$ ps. This value agrees quite well with the results of a recent two-dimensional vibrational echo study of a solution of NaBF $_4$. In this study the time constant at which a hydroxyl groups switches from the BF $_4^-$ ion to the oxygen atom of a nearby water molecule was observed to be 7 ± 1 ps.

Conclusions

We studied the hydrogen-bond dynamics of the hydration shell of the bromide anion using femtosecond spectral hole-burning spectroscopy. We find that at short delay times the spectral dynamics are governed by the vibrational relaxation with a time constant T_1 of 0.8 ± 0.1 ps of the O–H groups of water molecules that are hydrogen bonded to other water molecules. The O–H groups that are hydrogen bonded to Br $^-$ anions show a much slower vibrational relaxation with a time constant T_1 of 3.1 ps for a solution of 5 m LiBr. This latter vibrational relaxation time constant increases slightly with the concentration of dissolved salt to a value of 3.8 ± 0.2 ps for a solution of

R. L. A. Timmer et al. Hydrogen-bond fluctuations of the hydration shell of the bromide anion
15 m LiBr. Due to the large difference in vibrational lifetime, the spectral dynamics observed at
delays >4 ps are solely due to the spectral dynamics of the water molecules forming $\text{O-H}\cdots\text{Br}^-$
hydrogen bonds in the hydration shell of Br^- .

From the measurement of the first spectral moment of the spectral holes, we deduce that the
spectral dynamics of the $\text{O-H}\cdots\text{Br}^-$ oscillators are governed by a component with a time constant
of 4.3 ± 0.3 ps. This time constant shows a negligible dependence on the concentration of dis-
solved salt and on the nature of the cation. The process with a time constant of 4.3 ± 0.3 ps leads to
a complete spectral equilibration of the absorption band of the $\text{O-H}\cdots\text{Br}^-$ oscillators. This process
likely represents a complete reorganization of the hydration shell. The value of the time constant of
the reorganization agrees very well with the calculated time constant of the $\text{O-H}\cdots\text{Br}^-$ hydrogen-
bond correlation function obtained with molecular dynamics simulations.^{31,32} For a fraction of
the hydroxyl groups, the reorganization results in a switch of the $\text{O-H}\cdots\text{Br}^-$ hydrogen bond to
an $\text{O-H}\cdots\text{O}$ hydrogen bond. This switch represents an effective relaxation channel for the O-H
stretch vibration, and in most cases will lead to the departure of the water molecule from the hy-
dration shell. The increase of T_1 of the $\text{O-H}\cdots\text{Br}^-$ oscillators with increasing LiBr concentration
can thus be explained from the fact that the fraction of water molecules for which the hydrogen
bond switches to $\text{O-H}\cdots\text{O}$ decreases with increasing salt concentration.

Acknowledgement

This work is part of the research program of the "Stichting voor Fundamenteel Onderzoek der Ma-
terie (FOM)", which is financially supported by the "Nederlandse organisatie voor Wetenschap-
pelijk Onderzoek (NWO)".

References

- (1) Eisenberg D.; Kauzmann W., *The Structure and Properties of Water* (Oxford University Press,
New York, 1969).

- (2) Hadži, D.; Bratos S., in *The Hydrogen Bond*, edited by P. Schuster, Zundel G., Sandorfy C. (Elsevier, Amsterdam, 1976), Vol. 2, Chap. 12.
- (3) Rey, R.; Moller, K. B.; Hynes, J. T. *J. Phys. Chem. A* **2002**, *106*, 11993.
- (4) Lawrence, C. P.; Skinner, J. L. *J. Chem. Phys.* **2003** *118*, 264.
- (5) Corcelli, S. A.; Lawrence, C. P.; Skinner, J. L. *J. Chem. Phys.* **2004**, *120*, 8107.
- (6) Auer, B.; Kumar, R.; Schmidt, J. R.; Skinner, J. L. *Proc. Natl. Acad. Sci. USA* **2007**, *104*, 14215.
- (7) Gale, G. M.; Gallot, G.; Hache, F.; Lascoux, N.; Bratos, S.; Leicknam, J.-C. *Phys. Rev. Lett.* **1999**, *82*, 1086.
- (8) Woutersen, S.; Bakker, H. J. *Phys. Rev. Lett.* **1999**, *83*, 2077.
- (9) Stenger, J.; Madsen, D.; Hamm, P.; Nibbering, E. T. J.; Elsaesser, T. *Phys. Rev. Lett.* **2001** *87*, 027401.
- (10) Stenger, J.; Madsen, D.; Hamm, P.; Nibbering, E. T. J.; Elsaesser, T. *J. Phys. Chem. A* **2002**, *106*, 2341.
- (11) Yeremenko, S.; Pshenichnikov, M. S.; Wiersma, D. A. *Chem. Phys. Lett* **2003**, *369*, 107.
- (12) Fecko, C. J.; Eaves, J. D.; Loparo, J. J.; Tokmakoff, A.; Geissler, P. L. *Science* **2003**, *301*, 1698.
- (13) Asbury, J. B.; Steinel, T.; Stromberg, C.; Corcelli, S. A.; Lawrence, C. P.; Skinner, J. L.; Fayer, M. D. *J. Phys. Chem. A* **2004**, *108*, 1107.
- (14) Fecko, C. J.; Loparo, J. J.; Roberts, S. T.; Tokmakoff, A. *J. Chem. Phys.* **2005**, *122*, 054506.
- (15) Loparo, J. J.; Roberts, S. T.; Tokmakoff, A. *J. Chem. Phys.* **2006**, *125*, 194522.
- (16) Laage, D.; Hynes, J. T. *Science* **2006**, *311*, 832.

- (17) Mikenda, W. *J. of Mol. Struct.* **1986**, *147*, 1–15.
- (18) Walrafen, G. E. *J. Chem. Phys.* **1962**, *36*, 1035.
- (19) Bergström, P.-A.; Lindgren, J. *J. Phys. Chem.* **1991**, *95*, 8575-8580.
- (20) Kropman, M. F.; Bakker, H. J. *Science* **2001**, *291*, 2118.
- (21) Kropman, M. F.; Bakker, H. J. *J. Chem. Phys.* **2001**, *115*, 8942.
- (22) Park S.; Fayer, M. D. *Proc. Natl. Acad. Sci. USA* **2007**, *104*, 16731.
- (23) Park, S.; Moilanen, D. E.; Fayer M. D. *J. Phys. Chem. B* **2008**, *112*, 5279.
- (24) Woutersen, S.; Bakker, H. J. *Nature* **1999**, *402*, 507.
- (25) Timmer, R. L. A.; Bakker, H. J. *J. Chem. Phys.* **2007**, *126*, 154507.
- (26) Woutersen, S.; Emmerichs, U.; Nienhuys, H.-K.; Bakker, H. J. *Phys. Rev. Lett.* **1998**, *81*, 1106.
- (27) Moilanen, D. E.; Wong, D.; Rosenfeld, D. E.; Fenn, E. E.; Fayer, M. D. *Proc. Natl. Acad. Sci. USA* **2009**, *109*, 375.
- (28) Kropman, M. F.; Nienhuys, H.-K.; Bakker, H. J. *Phys. Rev. Lett.* **2002**, *88*, 77601.
- (29) Omta, A. W.; Kropman, M. F.; Woutersen, S.; Bakker, H. J. *Science* **2003**, *273*, 347.
- (30) Omta, A. W.; Kropman, M. F.; Woutersen, S.; Bakker H. J. *J. Chem. Phys.* **2003**, *119*, 12457.
- (31) Guarda, E.; Laria, D.; Mart, J. *J. Phys. Chem. B* **2006**, *110*, 6332.
- (32) Chowdhuri S.; Chandra, A. *J. Phys. Chem. B* **2006**, *110*, 9674.
- (33) Laage D.; Hynes, J. T. *Proc. Natl. Acad. Sci. USA* **2007**, *104*, 11167.
- (34) Kropman, M. F.; Bakker H. J. *J. Am. Chem. Soc.* **2004**, *126*, 9135.

(35) Bakker H. J. *Chem. Rev.* **2008**, *108*, 1456.

(36) Hertz, H.G. in *The Chemical Physics of Solvation, Part B Spectroscopy of Solvation*, ed. R.R. Dogonadze, E. Kálmán, A.A. Kornyshev, and J. Ulstrup; Elsevier: Amsterdam, 1987.

(37) Raugei, S.; Klein, M. L. *J. Chem. Phys.* **2002**, *116*, 196.

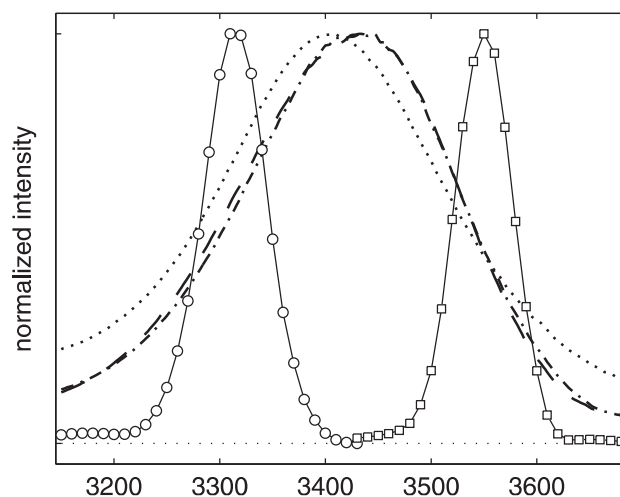


Figure 1: Linear absorption spectra of the O–H stretch vibration of HDO for different solutions. The dotted curve represents the absorption spectrum of a solution of 2% HDO in D_2O . The dash-dotted curve represents the absorption spectrum of a solution of 5 molal LiBr in 2% HDO: D_2O , and the dashed curve the absorption spectrum of a solution of 15 molal LiBr in 2% HDO: D_2O . Also shown are the pump spectra used in the measurement of the spectral dynamics shown in Figures 2-6.

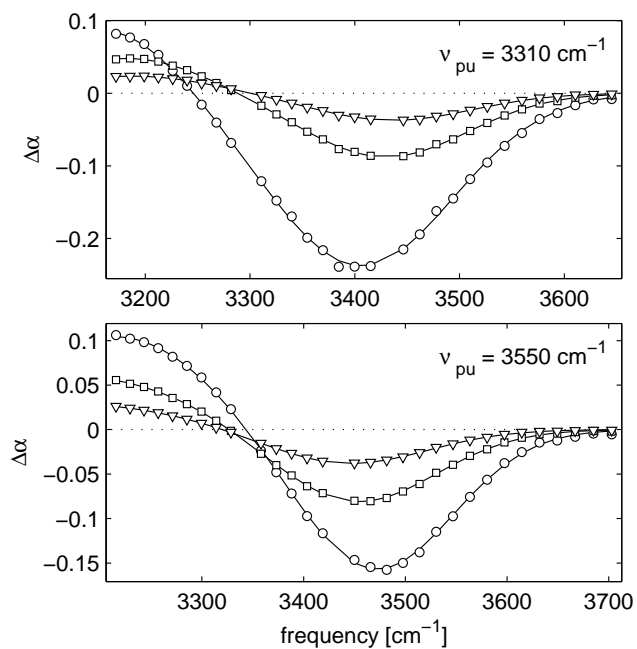


Figure 2: Transient spectra measured at different delay times for the a solution of 5 molal LiBr in 2% HDO:D₂O. Transient spectra are shown at delay times of 0.5 (circles), 1 (squares) and 2 (triangles) ps. The lines are obtained by fitting the spectra to a sum of two gaussians with opposite sign.

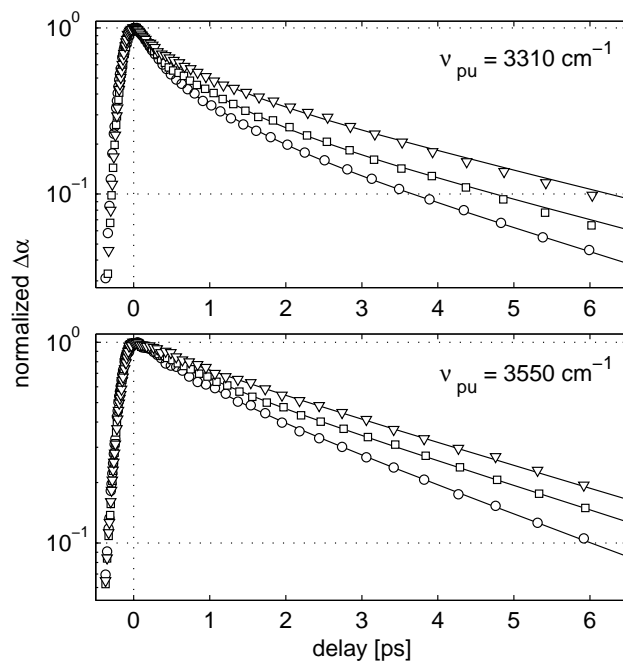


Figure 3: Bleaching signal as a function of delay measured at the maximum of the bleaching for solutions of 5 (circles), 10 (squares), and 15 (triangles) molal LiBr in 2% HDO:D₂O. The transients in the upper and lower panel are fitted with a bi-exponential decay with the same two time constants for each concentration. The two time constants represent the vibrational lifetimes T_1 of the O–H···O and the O–H···Br[−] oscillators.

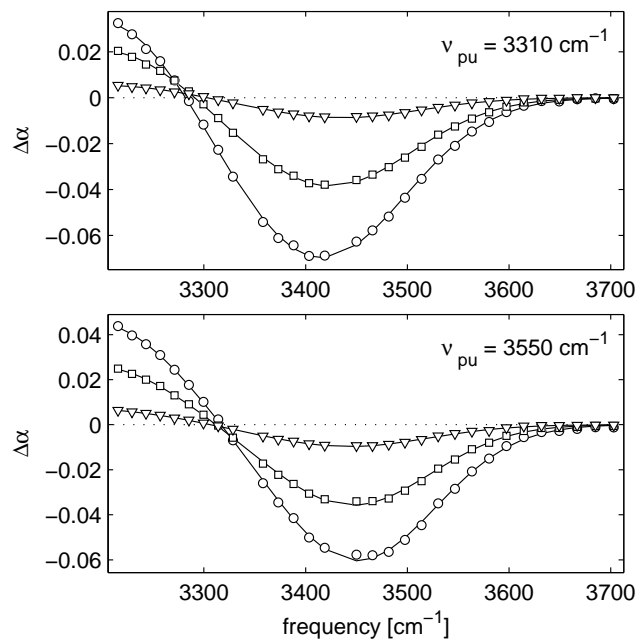


Figure 4: Transient spectra measured at different delay times for a solution of 15 molal LiBr in 2% HDO:D₂O. Transient spectra are shown at delay times of 4 (circles), 6 (squares) and 12 (triangles) ps. The lines are obtained by fitting the spectra to a sum of two Gaussians with opposite sign.

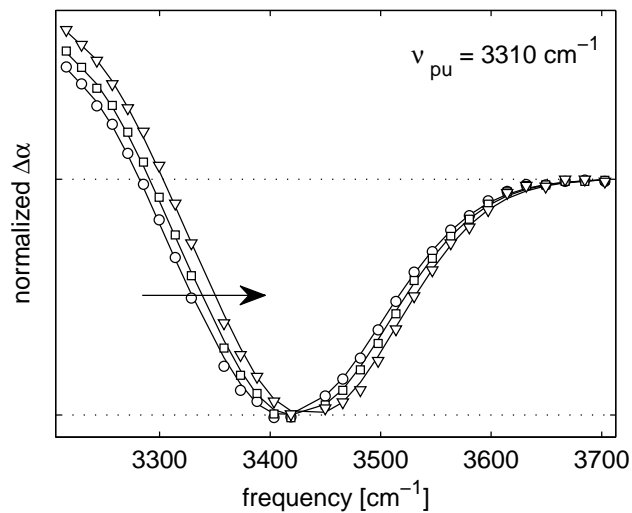


Figure 5: Same as the top panel of Figure 4, but normalized to the maximum bleaching signal to clarify the spectral diffusion.

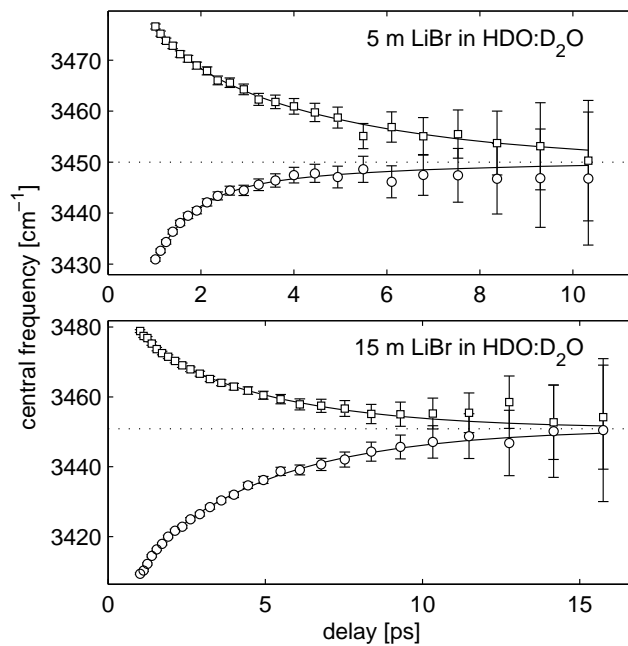


Figure 6: Spectral diffusion shown by the position of the central frequency (first moment) of the bleach signal ($\Delta\alpha < 0$) for solutions of 5 molal LiBr (upper panel) and 15 molal LiBr (lower panel) in 2% HDO:D₂O. Circles and squares denote red and blue pump frequencies. The lines represent bi-exponential fits of which the parameters are shown in Table 1.

Table 1: Time constants of the bi-exponential fits to the first moments observed for different solutions containing Br^- ions. The amplitudes $A_1(\text{red})$ and $A_2(\text{red})$ refer to the case where the absorption band is pumped in the red wing at 3310 cm^{-1} , and the amplitudes $A_1(\text{blue})$ and $A_2(\text{blue})$ correspond to the case where absorption band was pumped in the blue wing at 3550 cm^{-1} .

	$\nu_{\text{c,OH-Br}}$	$A_1(\text{red})$	$A_1(\text{blue})$	τ_1	$A_2(\text{red})$	$A_2(\text{blue})$	τ_2
5 m LiBr	3450 cm^{-1}	$-47\pm 4\text{ cm}^{-1}$	$19\pm 2\text{ cm}^{-1}$	$0.8\pm 0.1\text{ ps}$	$-7.5\pm 1\text{ cm}^{-1}$	$27\pm 3\text{ cm}^{-1}$	$4.2\pm 0.4\text{ ps}$
10 m LiBr	3449 cm^{-1}	$-45\pm 4\text{ cm}^{-1}$	$20\pm 4\text{ cm}^{-1}$	$0.9\pm 0.1\text{ ps}$	$-11\pm 1\text{ cm}^{-1}$	$26\pm 2\text{ cm}^{-1}$	$4.3\pm 0.3\text{ ps}$
15 m LiBr	3451 cm^{-1}	$-25\pm 2\text{ cm}^{-1}$	$20\pm 2\text{ cm}^{-1}$	$0.6\pm 0.2\text{ ps}$	$-46\pm 4\text{ cm}^{-1}$	$30\pm 3\text{ cm}^{-1}$	$4.3\pm 0.2\text{ ps}$
6 m NaBr	3460 cm^{-1}	$-28\pm 2\text{ cm}^{-1}$	$2.7\pm 1\text{ cm}^{-1}$	$0.9\pm 0.1\text{ ps}$	$-2\pm 0.5\text{ cm}^{-1}$	$7\pm 2\text{ cm}^{-1}$	$4.7\pm 0.4\text{ ps}$